

Article

The Catalytic Activities of Carbocyclic Fused Pyridineimine Nickel Complexes Analogues in Ethylene Polymerization by Modeling Study

Arfa Abrar Malik ^{1,2,†}, Wenhong Yang ^{1,2,*}, Zhifeng Ma ¹  and Wen-Hua Sun ^{1,2,*} 

¹ Key laboratory of Engineering Plastics and Beijing National Laboratory for Molecular Science, Institute of Chemistry, Chinese Academy of Sciences, Beijing 100190, China; arfamalik@iccas.ac.cn (A.A.M.); mazhifeng@iccas.ac.cn (Z.M.)

² University of Chinese Academy of Sciences, Beijing 100049, China

* Correspondence: whyang@iccas.ac.cn (W.Y.); whsun@iccas.ac.cn (W.-H.S.)

† Arfa Abrar Malik and Wenhong Yang contributed equally to this work.

Received: 22 May 2019; Accepted: 10 June 2019; Published: 12 June 2019



Abstract: In this work, two carbocyclic fused pyridineimine nickel analogue systems (Ni1 and Ni2) with different fused member rings were investigated to reveal the relationship between catalyst structure and reaction activity. Multiple linear regression analysis was performed by means of five electronic descriptors and two steric descriptors, including the Hammett constant (F), effective net charge (Q_{eff}), energy difference (ΔE), HOMO–LUMO energy gap ($\Delta\varepsilon_1$, $\Delta\varepsilon_2$), open cone angle (θ), and bite angle (β). Very good values of correlation coefficient (R^2) over 0.938 were obtained by using a combination of effective net charge (Q_{eff}) and open cone angle (θ) for both individual analysis and comparisons between analogue systems. By analyzing the contribution of descriptors, it indicates that the dominant descriptor is effective net charge (Q_{eff}) in the Ni1 system and open cone angle (θ) in Ni2 systems, respectively. This may explain the different variation trends of catalytic activities in two Ni complexes systems as a function of substituents.

Keywords: Catalytic activity; Nickel complexes; Multiple linear regression analysis; Ethylene polymerization; Modeling and simulation

1. Introduction

Due to the extensive number of applications inside film, isolated cable, engineering plastics and so forth, polyethylene has been playing an imperative role in our daily life and industry [1–3]. The physical and mechanical properties of polyethylene mainly depend on the structure of the product, which can be adjusted by a transition metal complex catalyst through decreasing the activation energy barrier during ethylene oligomerization and polymerization [4,5]. Catalytic activity is the most important property among the catalytic performance of transition metal complexes. Many achievements have been obtained previously by increasing the reaction activity of the complex, the modification of ligands, the alternation of substitutions on ligands, as well as the design of a new structure for ligands [6–10]. However, the potential principle of a transition metal complex with high catalytic activity still needs to be clarified at the molecular level.

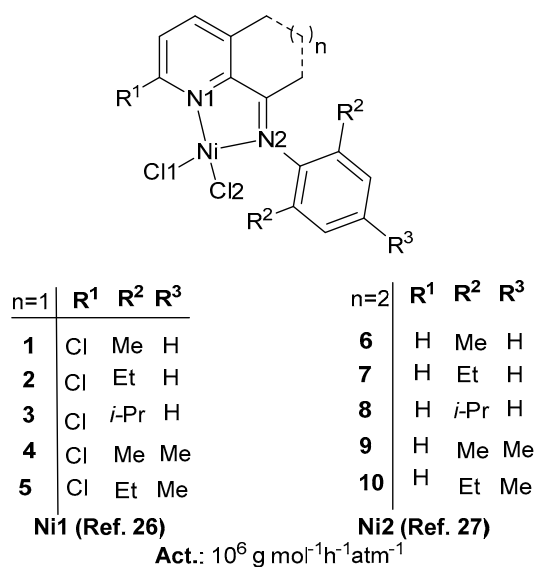
Generally, catalytic activity is fundamentally related to the structure of catalyst, such as the electronic and steric effects. The electron donating and withdrawing ability of substituents describes the electronic effect [11,12], while the steric effect is actually associated with bond length, bond angle, size of the substituents, and atomic radii of transition metal [13–15]. In preceding reports, the catalytic activities for Fe, Co and Ni complex systems are investigated quantitatively from the perspective of the electronic effect by the correlation with effective net charge on the central metal atom (Q_{eff}) [16–18],

Highest occupied molecular orbital (HOMO) and lowest unoccupied molecular orbital (LUMO) energy gaps ($\Delta\varepsilon$) between complex and ethylene [19], and the energy difference between the two spin states (ΔE) [19], respectively.

Besides the electronic effect, the impact of the steric effect on the catalytic activity is also investigated in terms of the open cone angle (θ) and bite angle (β). The former describes the space around the central metal in the complex to accommodate the approaching ethylene monomer [20], and the latter is the coordination angle of the metal with bonded nitrogens [21,22]. By using the multiple linear regression analysis (MLRA) method, the catalytic activities of azacyclic-6-aryliminopyridylmetal (Fe, Co, and Cr) complexes are predicted by considering both the electronic (Q_{eff} and Hammett constant F) and steric effects (θ and β) [20]. Furthermore, modified MLRA is carried out to investigate the variation of activities between 2-imino-1,10-phenanthrolinylmetal analogues, by using the variation of descriptors as independent variables and variation of the activity as a dependent variable. The calculation results exhibit quite good correlations for the analogues containing different substituents [23].

Nickel complex pre-catalysts can produce polyethylene with a hoisted level of branches and high molecular weight [24,25]. Herein, two Ni complexes systems are selected from our previous experimental reports, with the structure shown in Scheme 1. We defined the two systems as Ni1 and Ni2, respectively. Clearly, these two systems have very similar frameworks of ligands, and the same substituents of R^2 and R^3 . The differences lie in the presence of the R^1 substituent in the Ni1 system, and the different numbers of the carbocyclic fused rings, there is a six-membered ring in the Ni1 system and a seven-membered ring in the Ni2 system. Accordingly, the variations of the catalytic activities present very different trends as shown in Figure 1. For the Ni1 system, the activities present increasing trend for complexes 1–3 and complexes 4–5. Conversely, there is a decreasing trend of activities for both complexes 6–8 and complexes 9–10 in the Ni2 system. The catalytic activities are listed in Table 1 together with the reaction conditions [26,27].

Although the experimental conditions may change the absolute value of the activity and the variation trend remains same. Therefore, in this study, the main attentions focus on the different variation trend of catalytic activities for the two Ni analogue systems. MLRA is performed to find the key factors of the catalytic activity for each Ni system. Based on previous reports, five electronic and two steric descriptors are selected, including Hammett constants (F), effective net charge (Q_{eff}), energy difference (ΔE), HOMO–LUMO energy gap ($\Delta\varepsilon_1$, $\Delta\varepsilon_2$), the open cone angle (θ), and bite angle (β) [28]. Different numbers and combinations of descriptors are tried to get better correlation with catalytic activity. The main purpose of this study is to explain the reason causing the opposite variation trend of activities for Ni1 and Ni2 systems at a molecular level.



Scheme 1. The structure of carbocyclic fused pyridineimine nickel complexes.

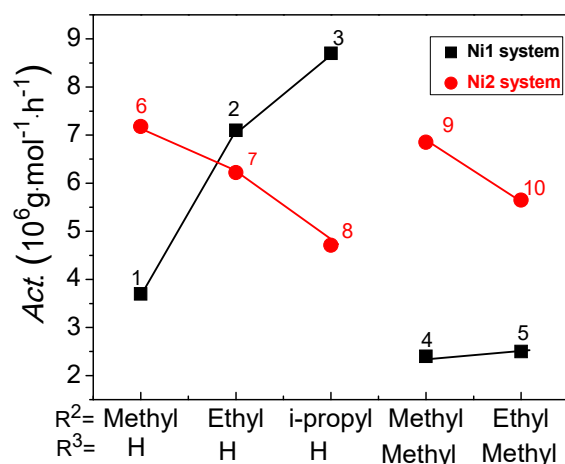


Figure 1. The variation of experimental activities as a function of R^2 and R^3 substituents for Ni1 and Ni2 complexes, respectively.

Table 1. The experimental catalytic activities and reaction conditions for the nickel complexes.

Complex	Co-catalyst	P ^a	Ratio ^b	T ^c	T ^d	Precatalyst	Activity ^e
1	EASC	10	400	20	30	5 μ mol	3.7
2	EASC	10	400	20	30	5 μ mol	7.1
3	EASC	10	400	20	30	5 μ mol	8.7
4	EASC	10	400	20	30	5 μ mol	2.4
5	EASC	10	400	20	30	5 μ mol	2.5
6	EASC	10	800	20	30	3 μ mol	7.18
7	EASC	10	800	20	30	3 μ mol	6.22
8	EASC	10	800	20	30	3 μ mol	4.71
9	EASC	10	800	20	30	3 μ mol	6.85
10	EASC	10	800	20	30	3 μ mol	5.65

^a atm of ethylene; ^b co-catalyst/catalyst; ^c reaction temperature ($^{\circ}$ C); ^d reaction time (min); ^e 10^6 g·mol⁻¹·h⁻¹.

2. Results and Discussion

Carbocyclic fused pyridineimine nickel complexes were selected as model to investigate the catalytic activities as shown in Scheme 1. It is clear that the complex Ni2 system is the seven-member ring analogue of the Ni1 system. Additionally, the R^1 substituent connected with the quinoline ring is another variation for consideration. As shown in experiments [26,27], Ni1 and Ni2 complexes were synthesized by a one pot reaction and a step by step method, respectively, via the formation of ligands. The geometry is different, it is trigonal bipyramidal for the Ni1 system, and a distorted square-pyramidal geometry for the Ni2 system. In the present study, we firstly explore the catalytic activities of Ni1 and Ni2 systems individually by MLRA. Then the difference of catalytic activities between the Ni1 and Ni2 systems (Ni1–Ni2) is further investigated by using a modified MLRA.

2.1. Predicted Activity of Ni1 System

To validate the parameters in calculation, the geometry of complex 3 was optimized and compared with its experimental crystal structure. The values of bond lengths and bond angles from calculation and experiment are listed in Table 2. It is clear that the standardized deviations (δ) for bond length and bond angle at triplet state are smaller than that at singlet state. Meanwhile, the structure at triplet has the lower value of optimized energy (ΔE). Therefore, we selected the triplet state for the following calculations for the Ni1 model system.

The values of seven descriptors for each complex were calculated on the basis of optimized structures and listed in Table 3. The values of the Hammett constant (F) were taken from literature which corresponds to the type of substituent [29]. As to the effective net charge (Q_{eff}), the values

decreased from complexes **1** to **3** corresponding to the change of the R² substituent from methyl to *i*-propyl. The presence of an electron donating group caused high electron density on the central metal, resulting in the reduction of positive charge value on the central metal atom. There were higher values of effective net charge in complexes **4** and **5** compared to complexes **1** and **2**, respectively. It means that the introduction of the substituent on the para-position of the phenyl ring induces a positive effect on the effective net charge, which is different from the substituent on the ortho-position. Meanwhile, the effective net charges present the same descent trend from complexes **4** to **5**. By keeping this variation of catalytic activities in mind, it is clear that the catalytic activities present a clear decreasing trend with Q_{eff} .

Table 2. The comparisons of bond lengths and bond angles between calculated geometry and experimental data for complex **3** along with standard deviations (δ) and energy variations (ΔE).

Complex 3	Experiment	Singlet	Triplet
Bond Length [Å]			
Ni(1)-N(1)	2.077	1.969	2.047
Ni(1)-N(2)	2.054	1.944	2.028
Ni(1)-Cl(1)	2.278	2.168	2.201
Ni(1)-Cl(2)	2.324	2.158	2.201
Ni(2)-C(9)	1.292	1.320	1.301
N(2)-C(10)	1.460	1.439	1.444
N(1)-C(1)	1.327	1.343	1.333
N(1)-C(5)	1.379	1.379	1.363
δ		3.490	1.958
Bond Angles [°]			
N(2)-Ni(1)-N(1)	79.8	82.43	80.93
N(2)-Ni(1)-Cl(1)	102.5	96.35	108.7
N(1)-Ni(1)-Cl(1)	89.4	95.71	81.73
N(2)-Ni(1)-Cl(2)	107.6	96.45	111.7
N(1)-Ni(1)-Cl(2)	89.6	97.20	94.3
Cl(1)-Ni(1)-Cl(2)	149.2	94.25	133.2
δ		16.94	7.32
ΔE [kcal·mol ⁻¹]		4.83	0

Table 3. The values of Hammett constant (F), effective net charge (Q_{eff}), open cone angle (θ), bite angle (β), energy difference (ΔE) and HOMO–LUMO energy gap ($\Delta\epsilon_1$, $\Delta\epsilon_2$) together with experimental catalytic activities for complexes **1–5**.

Complex No.	F	Q [e]	θ [°]	β [°]	Descriptors			Activity (10 ⁶ g·mol ⁻¹ ·h ⁻¹)
					ΔE [kcal/mol]	$\Delta\epsilon_1$ [kcal/mol]	$\Delta\epsilon_2$ [kcal/mol]	
1	0.47	0.489	245.8	80.6	1.45	65.87	100.71	3.7
2	0.45	0.483	243.5	80.8	2.67	66.42	100.74	7.1
3	0.53	0.482	230.4	80.9	4.38	66.48	100.95	8.7
4	0.45	0.493	245.6	80.6	1.38	66.63	98.96	2.4
5	0.43	0.489	243.3	80.8	2.60	66.88	99.00	2.5

Regarding the effect of substituents on the steric descriptors, the variation trends of open cone angle (θ) and bite angle (β) exhibited consistency with each other. According to the change of R² substituents from methyl to *i*-propyl, the values of open cone angle (θ) gradually reduced from 245° to 230° for complexes **1–3**. The steric hindrance surrounding the central metal atom increased due to the presence of big size substituents, resulting in a decrease of space to accommodate the incoming ethylene. For complexes **4** and **5**, the values of the open cone angle (θ) exhibited a slight decrease by the introduction of the R³ substituent in contrast to complexes **1** and **2**, respectively. This was owing to the para-position of R³ substituent, which was far from the central metal and had a tiny effect on the open cone angle. There was a clear decreasing correlation between the open cone angle (θ) and catalytic activities. This result is different from previous studies on Fe and Co complexes systems, but

in agreement with previous Ni complexes systems because of the bidentate nitrogen coordination framework [23]. For the bite angle (β) measured in N1–Ni–N2, it almost kept constant around 80° and an independence on the variation of substituents. Although the variations were very small, there were clear increasing trends for complexes 1 to 3 and complexes 4 to 5, as well as a function of substituents. The regular variation was attributed to the change of the open cone angle. Based on the framework of ligands in Ni complexes, a decrease in the open cone angle (θ) results in an increase in the bite angle (β) correspondingly.

The values of energy difference (ΔE) increased from 1.45 to 4.38 kcal/mol for complexes 1 to 3 according to the change of R^2 substituents. With the appearance of R^3 substituent, the energy differences (ΔE) slightly decreased in complexes 4 and 5 compared with that of complexes 1 and 2, respectively. The variation of energy difference (ΔE) presented regular increases with catalytic activities, which is in accordance to the previous report for Ni complexes [19]. For the HOMO–LUMO energy gap ($\Delta\epsilon_1$), the values almost keep constant around 66 kcal/mol, except the slightly bigger values in complexes 4 and 5 compared with complexes 1–3. This is due to the increased values of HOMO and LUMO orbital energy for the complexes containing electron-donating R^3 substituent. Similarly, in comparison with complexes 1–3, complexes 4 and 5 give low values for the descriptor of $\Delta\epsilon_2$.

In previous reports, the catalytic activities of 2-azacyclyl-6-aryliminopyridylmetal (Fe, Co and Cr) analogue complexes were investigated by MLRA using four descriptors, including two electronic descriptors (F , Q_{eff}), and two steric descriptors (θ , β). The obtained results show very good correlation with the coefficient value of R^2 over 0.93 [23]. Therefore, herein, we firstly chose four descriptors to investigate the catalytic activities for Ni1 complexes system as well. Since there are seven descriptors as candidate, there are 35 possible combination ways of taking four out of seven. Before performing MLRA for these combinations, the correlation coefficient values were calculated for each pair of descriptors to check the dependence between descriptors. The results were plotted into a matrix as in Figure S1a in the Supporting Information. It is clearly shown that the energy difference (ΔE) and HOMO–LUMO energy gap ($\Delta\epsilon_2$) had a high correlation with the R^2 value over 0.9. Therefore, the combinations of these two descriptors were eliminated and only the effective combinations with independent descriptors were considered for further calculations. There are 24 effective combinations, so MLRA was performed according to Equation (4) to correlate the calculated descriptors of each complex and the experimental catalytic activity.

The value of correlation ($R^2 = 1$) for all the different combinations of four descriptors was very good. Some of the combinations are selected and listed in Table 4. Although the correlation coefficient values were the same, the quality for each combination was different. We calculated the values of the weight factor for each four-descriptor model. As listed in Table S1 in the Supporting Information, the percentage of weight factor for most models was very close with the values around 4%, only the combination of $\Delta\epsilon_2$, F , Q , β and $\Delta\epsilon_2$, Q , θ , β gave a higher weight factor of 4.9%. As there are five complexes in Ni1 system, the very good correlations were high probably due to over fitting. Usually, the total number of descriptors should be less than half of the whole data set [30]. Based on this empirical rule of thumb, we performed further investigations on MLRA by selecting combinations of three and two descriptors.

Table 4. Selected values of correlation coefficient (R^2) for Ni1 complexes system by the combinations of four, three, two, and single descriptors.

Four Descriptors	Correlation Coefficient (R^2)	Three Descriptors	Correlation Coefficient (R^2)	Two Descriptors	Correlation Coefficient (R^2)	Single Descriptor	Correlation Coefficient (R^2)
F, Q, θ, β	1.00	$F, \Delta E, \beta$	0.998	$\Delta\epsilon_1, \Delta\epsilon_2$	0.980	Q	0.866
$\Delta E, Q, \theta, \beta$	1.00	$F, \Delta\epsilon_1, \Delta\epsilon_2$	0.987	Q, θ	0.961	β	0.605
$\Delta\epsilon_1, Q, \theta, \beta$	1.00	$\Delta E, Q, \theta$	0.985	$Q, \Delta\epsilon_2$	0.955	$\Delta\epsilon_2$	0.563
$\Delta\epsilon_2, Q, \theta, \beta$	1.00	$\Delta E, \Delta\epsilon_1, \beta$	0.963	$Q, \Delta\epsilon_1$	0.951	ΔE	0.549

There were 28 effective combinations of the three descriptors, and 27 combinations presented a very high correlation with the R^2 value over 0.9. When the number of descriptors was reduced to two, 11 out of 20 effective combinations gave good R^2 values. Selected combinations of three and two descriptors exhibiting high correlations are listed in Table 4. The linear fitting was also performed individually for each descriptor to check its impact on catalytic activities. It is found in Table 4 that among all the descriptors, the effective net charge (Q_{eff}) exhibited the highest correlation with the R^2 value of 0.866. This means that the effective net charge (Q_{eff}) is the dominant factor to determine the catalytic activity in the Ni1 complexes system.

In addition to the results listed in Table 4, the results from the rest combinations of four, three, two and single descriptors are tabulated in the Table S2. The calculated coefficient values (m_i) for the fitting Equation (4) by two descriptors are listed in Table S3.

2.2. Predicted Activity of Ni2 System

The catalytic activities of the Ni2 system were investigated in the same way as for the Ni1 system. The calculated geometry of complex 6 was compared with the experimental structure as shown in Table S4. It is clear that at the triplet state, the optimized energy is lower, and the geometry is closer to the experimental structure, as indicated by the lower standardized deviations of bond lengths and bond angles. Therefore, we still selected the triplet state for the analysis of the Ni2 complexes system. Based on the optimized geometries, the values of seven descriptors for complexes of this series were calculated and shown in Table 5.

Table 5. The values of Hammett constant (F), effective net charge (Q_{eff}), open cone angle (θ), bite angle (β), energy difference (ΔE) and HOMO–LUMO energy gap ($\Delta\varepsilon_1$, $\Delta\varepsilon_2$) together with experimental catalytic activities for complexes 6–10.

Complex No.	Descriptors							Activity ($10^6 \text{ g}\cdot\text{mol}^{-1}\cdot\text{h}^{-1}$)
	F	Q [e]	θ [°]	β [°]	ΔE [kcal/mol]	$\Delta\varepsilon_1$ [kcal/mol]	$\Delta\varepsilon_2$ [kcal/mol]	
6	0.08	0.396	253.2	80.1	1.09	70.59	96.20	7.18
7	0.06	0.398	251.0	80.2	0.86	70.91	96.13	6.22
8	0.14	0.403	244.2	80.3	0.00	70.53	95.88	4.71
9	0.06	0.403	253.2	80.2	1.04	71.54	95.32	6.85
10	0.04	0.402	248.4	80.2	0.82	71.79	95.19	5.65

Due to the variation of the R^1 substituent from Cl to H, the values of the Hammett constant (F) obviously decreased in the Ni2 system in contrast to the Ni1 system. Similarly, due to the R^1 substituent, the effective net charge showed an increasing trend for complexes 6–8 and complexes 9–10, respectively, different to the decreasing trend in the Ni1 system. Considering the different variation of catalytic activities in the Ni1 and Ni2 systems, the activity presents decreasing trend with the effective net charge (Q_{eff}) in both the Ni systems.

The values of the open cone angle (θ) gradually reduced from 253° to 244° , corresponding to the change of the R^2 substituents regarding complexes 6–8, and showing the same trend for complexes 9 to 10. Therefore, the catalytic activity presented an increasing correlation with the open cone angle (θ), which is in agreement with the previous study [20]. The variation of the bite angle (β) was very small, with the values of β keeping almost constant and independent on the substituents. There was only a slight increasing trend for complexes 6 to 8, and complexes 9 to 10, same as in the Ni1 system. Similar to the Ni1 analogue system, the energy difference (ΔE) presented an increasing trend corresponding to catalytic activity. The increased values of $\Delta\varepsilon_1$, and decreased values of $\Delta\varepsilon_2$, were also observed in complexes 9 and 10 compared with complexes 6 and 7, respectively.

The quantitative investigation of catalytic activities for the Ni2 system was performed by MLRA. In the same manner, many combinations of different numbers of descriptors were tried to get good fitting results, including four, three, and two descriptors. The correlation matrix in the Figure S1b

shows that there are high correlations between the descriptors of open cone angle (θ) and energy difference (ΔE), and between the two HOMO–LUMO energy gaps ($\Delta\varepsilon_1$ and $\Delta\varepsilon_2$). These two pairs of dependent descriptors were removed from all the combinations to maintain the effective combinations for analysis.

For 15 effective combinations of four descriptors, the correlation coefficient (R^2) values were very good. From the results of weight factors for each of the four-descriptors models, the combination of F , $\Delta\varepsilon_2$, θ , β showed the highest value of 9%. Out of 22 and 19 effective combinations of three and two descriptors, respectively, there were 20 and 14 combinations showing good correlation results with the R^2 value over 0.90. Some results are selected in Table 6. To check the influence of each single descriptor, the correlation values between the single descriptor and catalytic activities are calculated and listed in Table 6 as well. It can be seen that the open cone angle (θ) exhibits quite good correlation with catalytic activities with the coefficient R^2 value of 0.964. Meanwhile, the R^2 values of the energy difference (ΔE) and bite angle (β) are also good. Different from the results in the Ni1 system, the effective net charge (Q_{eff}) presented a very low correlation with the R^2 value of 0.127. It is clear that in the Ni2 system, open cone angle (θ) plays the dominated role, which is different from the major contribution of the effective net charge (Q_{eff}) in the Ni1 system.

Table 6. Selected correlation coefficient (R^2) values for Ni2 complexes system by using the combinations of four, three, two and single descriptors.

Four Descriptors	Correlation Coefficient (R^2)	Three Descriptors	Correlation Coefficient (R^2)	Two Descriptors	Correlation Coefficient (R^2)	Single Descriptor	Correlation Coefficient (R^2)
F, Q, θ, β	1.00	$F, \Delta E, \beta$	0.998	$F, \Delta E$	0.997	θ	0.964
$\Delta\varepsilon_1, Q, \theta, \beta$	1.00	F, Q, θ	0.993	$\Delta\varepsilon_1, \theta$	0.991	ΔE	0.814
$\Delta\varepsilon_2, Q, \theta, \beta$	1.00	$\Delta E, \Delta\varepsilon_1, \beta$	0.984	Q, θ	0.989	β	0.789
$F, \Delta\varepsilon_1, \theta, \beta$	1.00	$F, \Delta\varepsilon_1, \beta$	0.969	$\Delta\varepsilon_2, \theta$	0.988	$\Delta\varepsilon_1$	0.317

Besides the selected values listed in Table 6, other results of R^2 for the combinations of four, three, two, and single descriptors are listed in Table S5. Meanwhile, the calculated coefficient values (m_i) for equation (4) by two descriptors are summarized in Table S6.

2.3. Difference of Catalytic Activity between Ni1 and Ni2 Systems

In previous sections, the catalytic activities of Ni1 and Ni2 complexes systems were investigated individually by MLRA. In this section, modified MLRA is performed on the variation of catalytic activities between two analogue systems. According to Equation (5), the variation values of the seven descriptors between the Ni1 and Ni2 systems were calculated as independent variables, meanwhile the variation of catalytic activities was used as a dependent variable. The obtained results are listed in Table 7, where 1–6 means the variation between complex 1 in the Ni1 system and complex 6 in Ni2 system, with a similar meaning for others.

Table 7. The variation values of Hammett constant (F), effective net charge (Q_{eff}), open cone angle (θ), bite angle (β), energy difference (ΔE) and HOMO–LUMO energy gap ($\Delta\varepsilon_1$, $\Delta\varepsilon_2$) between Ni1 and Ni2 analogues together with the variation of catalytic activities ($\Delta Act.$).

Complex No.	Descriptors							$\Delta Act.$ ($10^6 \text{ g}\cdot\text{mol}^{-1}\cdot\text{h}^{-1}$)
	F	Q [e]	θ [°]	β [°]	ΔE [kcal/mol]	$\Delta\varepsilon_1$ [kcal/mol]	$\Delta\varepsilon_2$ [kcal/mol]	
1–6	0.39	0.093	−7.37	0.49	0.36	−4.72	4.51	−3.48
2–7	0.39	0.085	−7.57	0.61	1.81	−4.49	4.61	0.88
3–8	0.39	0.079	−13.83	0.62	4.38	−4.05	5.07	3.99
4–9	0.39	0.090	−7.59	0.41	0.35	−4.91	3.64	−4.45
5–10	0.39	0.087	−5.10	0.52	1.79	−4.91	3.81	−3.15

The variations of Hammett constants (F) kept constant around the value of 0.39, corresponding to the different results of the Hammett constants between Cl in the Ni1 system and H in the Ni2 system. Regarding the effective net charges, the variation values ranged from 0.079 to 0.093, which is about 20% of the absolute values in the Ni1 or Ni2 systems. For the steric effect, the variation values of the open cone angle (θ) were around -7° . The bigger values of θ in the Ni2 system may be due to the change of the carbocyclic fused member ring from six to seven. Comparatively, the variation of the bite angle (β) and energy differences (ΔE) were small, with values around 0.5° and 1.4 kcal/mol, respectively. The HOMO–LUMO energy gaps showed decreasing values around 4.4 kcal/mol for the descriptors of $\Delta\varepsilon_1$, and increasing values around 4.5 kcal/mol for the descriptors of $\Delta\varepsilon_2$, respectively. Regular variation trends with respect to the catalytic activities were observed for these descriptors.

Then, the modified MLRA was performed to investigate the variation in catalytic activities between the Ni1–Ni2 analogue by using different combinations of descriptors. Firstly, the correlations between each pair of descriptors were calculated as in Figure S1c. It is obviously shown that correlation coefficient values are high between the pairs of effective net charge (Q_{eff}) and energy difference (ΔE), open cone angle (θ) and HOMO–LUMO energy gap ($\Delta\varepsilon_1$), and the two HOMO–LUMO energy gaps ($\Delta\varepsilon_1$ and $\Delta\varepsilon_2$). Therefore, these three pairs of dependent descriptors were removed from all the possible combinations, leaving ten effective combinations. As in Table 8, the correlation values for all the combinations are very good with the R^2 value of 1. The results of the weight factors for each four-descriptor model showed the highest value of 11% by the combination of $\Delta\varepsilon_1$, F , Q , β .

Table 8. Correlation coefficient (R^2) values for Ni1–Ni2 analogue system for selected combinations of four, three, two and one descriptors.

Four Descriptors	Correlation Coefficient (R^2)	Three Descriptors	Correlation Coefficient (R^2)	Two Descriptors	Correlation Coefficient (R^2)	Single Descriptor	Correlation Coefficient (R^2)
F, Q, θ, β	1.00	$\Delta\varepsilon_2, Q, \theta$	0.995	$Q, \Delta\varepsilon_2$	0.995	$\Delta\varepsilon_1$	0.910
$\Delta\varepsilon_1, F, Q, \beta$	1.00	$F, Q, \Delta\varepsilon_2$	0.995	$Q, \Delta\varepsilon_1$	0.988	β	0.817
$F, \Delta E, \theta, \beta$	1.00	Q, θ, β	0.994	θ, β	0.989	ΔE	0.779
$F, \Delta\varepsilon_2, \theta, \beta$	1.00	$\Delta E, \theta, \beta$	0.989	Q, θ	0.938	Q	0.778

For the combination of three and two descriptors, out of 19 and 18 effective combinations, 18 and 15 combinations gave good correlation with the R^2 over 0.9, respectively. Selected good results for four, three, two descriptors are shown in Table 8. The correlations for each single descriptor were also checked, showing the good R^2 value of 0.910 by the descriptors of $\Delta\varepsilon_1$.

The correlation values for the rest combinations of three, two, and single descriptors are summarized in Table S7 for the Ni1–Ni2 analogue. The linear fitting coefficients values (w_1) by the combinations of two descriptors are illustrated in Table S8.

Clearly, there were several combinations of two descriptors that exhibited good correlation results for the Ni1 and Ni2 systems individually as well as for the Ni1–Ni2 analogue system, such as the combination of Q_{eff} and θ , Q and β , $\Delta\varepsilon_2$ and β . Herein, the combination of effective net charge (Q_{eff}) and open cone angle (θ) was selected, which give higher correlation results for all systems. The corresponding correlation coefficient values were 0.961, 0.989 and 0.938 for the Ni1 system, Ni2 system and Ni1–Ni2 analogue, respectively. The comparisons between the experimental and the calculated activities for each system are displayed in Figure 2.

As mentioned in the introductory section, regarding the structure of Ni1 and Ni2 systems, the different substituent of R^1 and size of the carbocyclic fused ring cause different variation trends in catalytic activities. In order to clarify the reason, the contributions of each descriptor on catalytic activities were calculated. Firstly, the calculated descriptors and the catalytic activities for each system were standardized by using Z–Score method, as listed in Table 9. By using Equation (6), the contributions of each descriptor were calculated and the obtained results are shown in Table 10. Clearly, in the Ni1 system, effective net charge (Q_{eff}) plays a dominant effect on the catalytic activities, with a contribution

value of 80.98%. However, different from the Ni1 system, the dominated factor becomes the open cone angle (θ) in the Ni2 system with a contribution value of 88.76%. The results indicate that, due to the presence of the substituent of Cl in Ni1 system, the electronic effect is a key factor in determining catalytic activity. While in the Ni2 system, because the carbocyclic fused member ring changed from six to seven and the R¹ substituent from Cl to H, the steric effect becomes the predominant factor. Therefore, the different dominant factor is the essential reason for the different variation of catalytic activities in the Ni1 and Ni2 systems.

Additionally, as in Figure 1, the R³ substituent deactivates the catalytic activity dramatically in the Ni1 system regarding complexes 4 and 5. But this is not the case in the Ni2 system, as complexes 9 and 10 are more active than complex 8. The main reason still comes from the different dominant descriptors in two systems. For the Ni1 system, the catalytic activities increased with the decreasing of Q_{eff} . Therefore, with the introduction of R³ substituent, the effective net charge values within complexes 4 and 5 increased, as seen from Table 3, leading to the lower catalytic activity of complexes 4 and 5. However, in the Ni2 system, because the dominant role on catalytic activity is the open cone angle (θ), the R³ substituent only causes very small decreases of θ in complexes 9 and 10, resulting in the slight reduce of their catalytic activities.

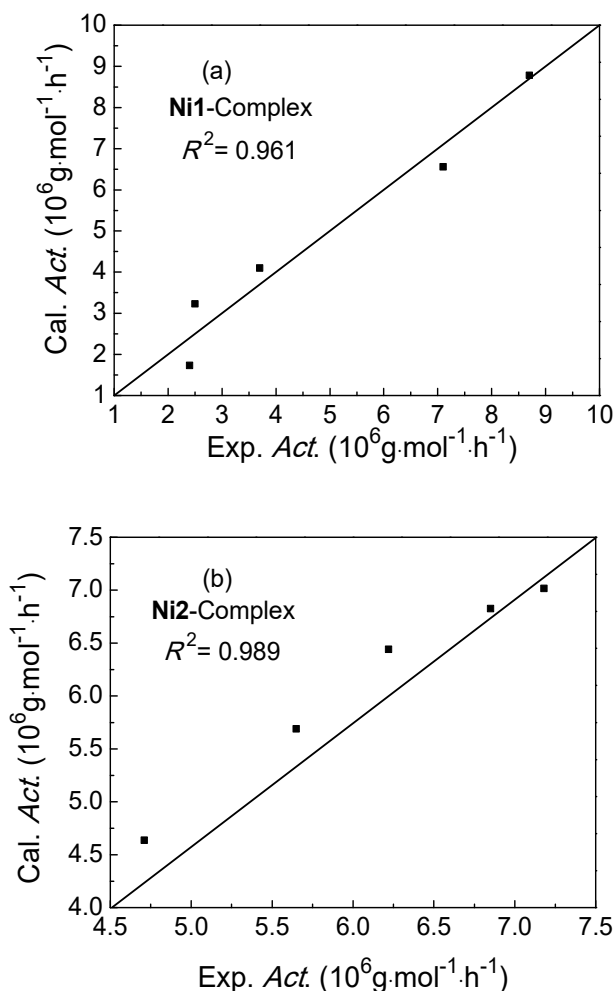


Figure 2. Cont.

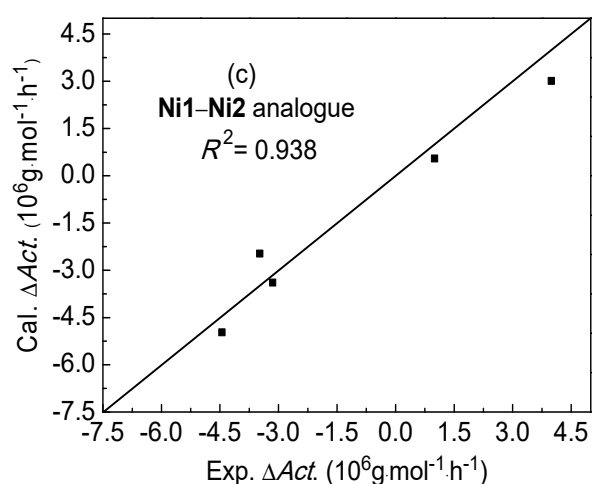


Figure 2. Comparisons between calculated and experimental activities of (a) Ni1 system, (b) Ni2 system, and (c) Ni1–Ni2 analogue system, by the descriptors of effective net charge (Q_{eff}) and open cone angle (θ).

Table 9. Standardized values of effective net charge (Q_{eff}) and open cone angle (θ) along with the values of catalytic activities of Ni1 complexes, Ni2 complexes and the analogue Ni1–Ni2 system.

Systems	Complex	Standardized Values		Activity
		Q	θ	
Ni1 system	1	0.39	0.63	−0.41
	2	−0.91	0.27	0.77
	3	−1.12	−1.75	1.33
	4	1.25	0.59	−0.86
	5	0.39	0.24	−0.83
Ni2 system	6	−1.37	0.84	1.07
	7	−0.74	0.27	0.09
	8	0.81	−1.53	−1.43
	9	0.81	0.83	0.73
	10	0.49	−0.42	−0.47
Ni1–Ni2 system	1–6	1.16	0.28	−0.62
	2–7	−0.33	0.22	0.59
	3–8	−1.46	−1.69	1.46
	4–9	0.60	0.21	−0.90
	5–10	0.03	0.97	−0.53

Table 10. Values of contribution of effective net charge (Q_{eff}) and open cone angle (θ) for Ni1 complexes, Ni2 complexes and the Ni1–Ni2 analogue system.

Complex System	Q [e]	θ [°]
Ni1 System	80.98	19.02
Ni2 System	11.23	88.77
Ni1–Ni2 analogue	65.26	34.74

3. Computational Details

In the present study, all the calculations were performed by density function theory (DFT) in a Dmol3 program [31,32]. The electronic structures of the molecular systems were optimized by the generalized gradient approximation (GGA) [33] and the Becke–Perdew (BP) [34] exchange correlation function combined with the double numerical basis sets with polarization functions (DNP) [31] using effective core potentials [35,36]. For geometry optimization, the convergence criteria of energy,

maximum force and displacement were 2.0×10^{-5} Hartree, 4.0×10^{-3} Hartree per Bohr and 5.0×10^{-3} Å, respectively. The convergence criterion for self-consistent field (SCF) calculation was 1.0×10^{-5} Hartree.

After the optimization of the complex, we calculated the descriptors of electronic and steric effects based on previous studies. The effective net charge (Q_{eff}) was calculated by Equation (1), which defines the difference of charge on central metal (Q_{CM}) and variation between two halogen atoms ($\Delta Q_{\text{halogens}}$) [17]. The HOMO–LUMO energy gaps ($\Delta\varepsilon_1$, $\Delta\varepsilon_2$) were actually the energy gap between complex's LUMO/HOMO ($E_{\text{LC}}/E_{\text{HC}}$) and ethylene's HOMO/LUMO orbitals ($E_{\text{HE}}/E_{\text{LE}}$), as calculated by Equations (2) and (3), respectively.

$$Q_{\text{eff}} = Q_{\text{CM}} - \Delta Q_{\text{halogens}} \quad (1)$$

$$\Delta\varepsilon_1 = E_{\text{LC}} - E_{\text{HE}} \quad (2)$$

$$\Delta\varepsilon_2 = E_{\text{LE}} - E_{\text{HC}} \quad (3)$$

Energy difference (ΔE) can be explained in terms of different optimized energy of Ni complex between singlet and triplet states [19]. The values of Hammett constant (F) were taken from literature [29], and depended on the type of substituents. The steric effect was calculated on the basis of an optimized structure of the complex. The bite angle (β) was measured as the angle of N1–Ni–N2 in complex. The open cone angle (θ) was obtained according to [20], accounting for the space to accommodate the incoming monomer.

To exhibit the association of structural descriptors with experimental activities, we chose the multiple linear regression analysis (MLRA) Equation (4):

$$\text{Act.} (10^a \text{ g}\cdot\text{mol}^{-1}\cdot\text{h}^{-1}) = \sum_{i=1}^N m_o + m_i X_i \quad (4)$$

where N represents the number of structural descriptors to establish the correlation with catalytic activities. In this study, we decided to choose four, three and two descriptors from the seven electronic and steric descriptors, so the value of N can be 2, 3 and 4. X_i is the value of each descriptor. The regression coefficients m_o and m_i were obtained by linear fitting analysis using the LINEST function in Microsoft Excel [37].

Similarly, the variation of catalytic activities between two series of complexes was analyzed by modified MLRA [23], which uses the variation of descriptors (ΔX_i) as the independent variables and the variation of catalytic activities ($\Delta \text{Act.}$) as the dependent variable, as shown in Equation (5):

$$\Delta \text{Act.} (10^a \text{ g}\cdot\text{mol}^{-1}\cdot\text{h}^{-1}) = \sum_{i=1}^N w_o + w_i \Delta X_i \quad (5)$$

where the value of N and regression coefficients w_o and w_i have same meaning as in Equation (4), which means that we also tried different numbers of descriptors to get the linear fitting equation for the variation of catalytic activities between two analogue systems, including the cases of four, three and two descriptors.

To analyze the contribution of each structural descriptor to the catalytic activity, the values of descriptors and activities were standardized by the Z-score method [38,39]. Contribution values were calculated for each descriptor by using the standardized values as shown in the equation (6):

$$\text{Contribution \%} = \frac{\sum_{j=1}^M \frac{|\bar{w}_j \cdot \Delta \bar{X}_j|}{\sum_{i=1}^N |\bar{w}_i \cdot \Delta \bar{X}_i|}}{M} \times 100\% \quad (6)$$

where, M is corresponding to the number of complexes in one series and N has the same meaning as in Equation (1) which describes the number of structural descriptors (2, 3 or 4). \bar{w} and $\Delta\bar{X}$ are the corresponding standardized values of linear fitting coefficients and variation of descriptors, respectively.

4. Conclusions

The variation of catalytic activities of carbocyclic fused pyridineimine nickel complex analogues (Ni1 and Ni2) were investigated quantitatively by the MLRA method. Based on our previous studies, five electronic and two steric descriptors were selected as the independent variables in linear fitting, including the Hammett constant (F), effective net charge (Q_{eff}), energy difference (ΔE), HOMO–LUMO energy gap ($\Delta\varepsilon_1$, $\Delta\varepsilon_2$), open cone angle (θ), and bite angle (β). Different numbers of descriptors were undertaken for each individual complexes system and the analogues (Ni1–Ni2) in order to obtain a high quality fitting model. The calculated results showed good values of correlation coefficient (R^2) by using different combinations of four, three, and two descriptors. Furthermore, the combination of effective net charge (Q_{eff}) and open cone angle (θ) gave good correlation results for both the individual and analogue systems. The corresponding correlation coefficient values (R^2) were 0.961, 0.989 and 0.938 for Ni1 system, Ni2 system and Ni1–Ni2 analogue system, respectively.

The contribution of each descriptor indicated that the effective net charge (Q_{eff}) plays the dominant role in order to determine the variation of catalytic activities in the Ni1 system. While in the Ni2 system, the open cone angle (θ) becomes the major factor due to the variation of the fused member-ring. This is the reason for the opposite variations of catalytic activities in Ni1 and Ni2 systems. Through this study, the major factor on catalytic activity of different Ni systems is clarified, which is helpful to provide guidance to predict and design new Ni complexes with desirable catalytic properties.

Supplementary Materials: The following are available online at <http://www.mdpi.com/2073-4344/9/6/520/s1>, Figure S1: The matrix of the correlations among the selected 7 descriptors and activity values for Ni1, Ni2 and Ni1–Ni2 systems, Table S1: The percentage values of weight factor for the various combinations of four descriptors of each system, Table S2: The correlation coefficient values (R^2) of MLRA using different sets of descriptors for Ni1 complexes, Table S3: Linear fitting coefficients values for Ni1 complex corresponding to combinations of two descriptors, Table S4: The comparisons of bond lengths and bond angles between calculated geometry and experimental crystal data for complex 6 along with standard deviation δ and energy variation ΔE , Table S5: The correlation coefficient values (R^2) of MLRA using different sets of descriptors for Ni2 complexes, Table S6: Linear fitting coefficients values for Ni2 complex corresponding to combinations of two descriptors, Table S7: The correlation coefficient values (R^2) of MLRA using different sets of descriptors for Ni1–Ni2 analogue, Table S8: Linear fitting coefficients values for Ni1–Ni2 analogue system corresponding to combinations of two descriptors.

Author Contributions: W.Y. and W.-H.S. conceived and designed the experiments; A.A.M. performed the experiments; Z.M. contributed analysis tools; and W.Y., A.A.M. and W.-H.S. analyzed the data and wrote the paper.

Acknowledgments: This work was financially supported by the National Natural Science Foundation of China (Grant Nos. 21871275 and 51861145303).

Conflicts of Interest: The authors declare no conflicts of interest.

References

1. Britovsek, G.J.P.; Gibson, V.C.; Wass, D.F. The search for new-generation olefin polymerization catalysts: Life beyond Metallocenes. *Angew. Chem. Int. Ed.* **1999**, *38*, 428–447. [[CrossRef](#)]
2. Resconi, L.; Cavallo, L.; Fait, A.; Piemontesi, F. Selectivity in propene polymerization with metallocene catalysts. *Chem. Rev.* **2000**, *100*, 1253–1345. [[CrossRef](#)] [[PubMed](#)]
3. Coates, G.W. Precise control of polyolefin stereochemistry using single-site metal catalysts. *Chem. Rev.* **2000**, *100*, 1223–1252. [[CrossRef](#)] [[PubMed](#)]
4. Ortega, D.E.; Arriagada, D.C.; Labbe, A.T. Mechanistic details of ethylene polymerization reaction using methyl nickel(II) catalysts. *Phys. Chem. Chem. Phys.* **2018**, *20*, 22915. [[CrossRef](#)]
5. Martinez, A.J.I.; Quijada, R.; Toro-Labbe, A. The mechanism of ethylene polymerization reaction catalyzed by group IVB metallocenes. A rational analysis through the use of reaction force. *J. Phys. Chem. C* **2012**, *116*, 21318–21325. [[CrossRef](#)]

6. Takeuchi, D. Recent progress in olefin polymerization catalyzed by transition metal complexes: New catalysts and new reactions. *Dalton Trans.* **2010**, *39*, 311–328. [[CrossRef](#)]
7. Sun, W.-H. Novel polyethylenes via late transition metal complex pre-catalysts. *Adv. Polym. Sci.* **2013**, *258*, 163–178. [[CrossRef](#)]
8. Gibson, V.C.; Redshaw, C.; Solan, G.A. Bis(imino)pyridines: Surprisingly reactive ligands and a gateway to new families of catalysts. *Chem. Rev.* **2007**, *107*, 1745–1776. [[CrossRef](#)]
9. Zhang, W.; Sun, W.-H.; Redshaw, C. Tailoring iron complexes for ethylene oligomerization and/or polymerization. *Dalton Trans.* **2013**, *42*, 8988–8997. [[CrossRef](#)]
10. Wang, Z.; Solan, G.A.; Zhang, W.; Sun, W.-H. Carbocyclic-fused N,N,N-pincer ligands as ring-strain adjustable supports for iron and cobalt catalysts in ethylene oligo-/polymerization. *Coord. Chem. Rev.* **2018**, *363*, 92–108. [[CrossRef](#)]
11. Piccolrovazzi, N.; Pino, P.; Consiglio, G.; Sironi, A.; Moret, M. Electronic effects in homogeneous indenylzirconium Ziegler-Natta catalysts. *Organometallics* **1990**, *9*, 3098–3105. [[CrossRef](#)]
12. Lee, I.-M.; Gauthier, W.J.; Ball, J.M.; Iyengar, B.; Collins, S. Electronic effects in Ziegler-Natta polymerization of propylene and ethylene using soluble metallocene catalysts. *Organometallics* **1992**, *11*, 2115–2122. [[CrossRef](#)]
13. Mohring, P.C.; Coville, N.J. Quantification of the influence of steric and electronic parameters on the ethylene polymerisation activity of (CpR)₂ZrCl₂/ethylaluminumoxane Ziegler-Natta catalysts. *J. Mol. Catal.* **1992**, *77*, 41–50. [[CrossRef](#)]
14. Mohring, P.C.; Coville, N.J. Homogeneous group 4 metallocene Ziegler-Natta catalysts: The influence of cyclopentadienyl-ring substituents. *J. Organomet. Chem.* **1994**, *479*, 1–29. [[CrossRef](#)]
15. Mohring, P.C.; Vlachakis, N.; Grimmer, N.E.; Coville, N.J. The influence of steric and electronic effects of substituents on the cyclopentadienyl ring on the behaviour of (CpR)₂TiCl₂ and (CpR)CpTiCl₂/Et₃Al₂Cl₃ catalysts in polymerization of ethane. *Organomet. Chem.* **1994**, *483*, 159–166. [[CrossRef](#)]
16. Chen, Y.; Yang, W.; Sha, R.; Fu, R.-D.; Sun, W.-H. Correlating net charges and the activity of bis(imino)pyridylcobalt complexes in ethylene polymerization. *Inorg. Chim. Acta* **2014**, *423*, 450–453. [[CrossRef](#)]
17. Yang, W.; Chen, Y.; Sun, W.-H. Assessing catalytic activities through modeling net charges of iron complex precatalysts. *Macromol. Chem. Phys.* **2014**, *215*, 1810–1817. [[CrossRef](#)]
18. Yang, W.; Chen, Y.; Sun, W.-H. Correlating cobalt net charges with catalytic activities of the 2-(Benzimidazolyl)-6-(1-aryliminoethyl) pyridylcobalt complexes toward ethylene polymerization. *Macromol. React. Eng.* **2015**, *9*, 473–479. [[CrossRef](#)]
19. Yang, W.; Yi, J.; Sun, W.-H. Revisiting benzylidenequinolinylnickel catalysts through the electronic effects on catalytic activity by DFT studies. *Macromol. Chem. Phys.* **2015**, *216*, 1125–1133. [[CrossRef](#)]
20. Yi, J.; Yang, W.; Sun, W.-H. Quantitative investigation of the electronic and steric influences on ethylene Oligo/Polymerization by 2-Azacyclyl-6-aryliminopyridylmetal (Fe, Co and Cr) complexes. *Macromol. Chem. Phys.* **2016**, *217*, 757–764. [[CrossRef](#)]
21. Casey, C.P.; Whiteker, G.T. The natural bite angle of chelating diphosphines. *Isr. J. Chem.* **1990**, *30*, 299–304. [[CrossRef](#)]
22. Van-Leeuwen, P.W.N.M.; Kamer, P.C.J.; Reek, J.N.H.; Dierkes, P. Ligand bite angle effects in metal-catalyzed C-C bond formation. *Chem. Rev.* **2000**, *100*, 2741–2769. [[CrossRef](#)] [[PubMed](#)]
23. Yang, W.; Ma, Z.; Sun, W.-H. Modeling study on the catalytic activities of 2-imino-1,10-phenanthrolylmetal (Fe, Co, and Ni) precatalysts in ethylene oligomerization. *RSC Adv.* **2016**, *6*, 79335–79342. [[CrossRef](#)]
24. Suo, H.; Solan, G.A.; Ma, Y.; Sun, W.-H. Development in compartmentalized bimetallic transition metal ethylene polymerization catalysts. *Coord. Chem. Rev.* **2018**, *372*, 101–116. [[CrossRef](#)]
25. Wang, Z.; Liu, Q.; Solan, G.A.; Sun, W.-H. Recent advances in Ni-mediated ethylene chain growth: N imine-donor ligand effects on catalytic activity, thermal stability and oligo-/polymerstructure. *Coord. Chem. Rev.* **2017**, *350*, 68–83. [[CrossRef](#)]
26. Yu, J.; Hu, X.; Zeng, Y.; Zhang, L.; Ni, C.; Hao, X.; Sun, W.-H. Synthesis, characterisation and ethylene oligomerization behaviour of N-(2-substituted-5,6,7-trihydroquinolin-8-ylidene) arylaminonickel dichlorides. *New J. Chem.* **2011**, *35*, 178–183. [[CrossRef](#)]
27. Huang, F.; Sun, Z.; Du, S.; Yue, E.; Ba, J.; Hu, X.; Liang, T.; Galland, G.B.; Sun, W.-H. Ring-tension adjusted ethylene polymerization by aryliminocycloheptapyridyl nickel complexes. *Dalton Trans.* **2015**, *44*, 14281–14292. [[CrossRef](#)]

28. Ahmed, S.; Yang, W.; Ma, Z.; Sun, W.-H. Catalytic activities of bis(pentamethylene)pyridyl(Fe/Co) complex analogues in ethylene polymerization by modeling method. *J. Phys. Chem. A* **2018**, *122*, 9637–9644. [[CrossRef](#)]
29. Hansch, C.; Leo, A.; Taft, R.W. A survey of hammett substituent constants and resonance and field parameters. *Chem. Rev.* **1991**, *91*, 165–195. [[CrossRef](#)]
30. Le, T.; Epa, V.C.; Burden, F.R.; Winkler, D.A. Quantitative structure—Property relationship modeling of diverse materials properties. *Chem. Rev.* **2012**, *112*, 2889–2919. [[CrossRef](#)]
31. Delley, B. An all-electron numerical method for solving the local density functional for polyatomic molecules. *J. Chem. Phys.* **1990**, *92*, 508–517. [[CrossRef](#)]
32. Delley, B. From molecules to solids with the Dmol³ approach. *J. Chem. Phys.* **2000**, *113*, 7756–7764. [[CrossRef](#)]
33. Becke, A.D. A multicenter numerical integration scheme for polyatomic molecules. *J. Chem. Phys.* **1988**, *88*, 2547–2553. [[CrossRef](#)]
34. Perdew, J.P.; Wang, Y. Accurate and simple analytic representation of the electron-gas correlation energy. *Phys. Rev. B Condens. Matter Mater. Phys.* **1992**, *45*, 13244–13249. [[CrossRef](#)]
35. Dolg, M.; Wedig, U.; Stoll, H.; Preuss, H. Energy-adjusted ab initio pseudopotentials for the first row transition elements. *Chem. Phys.* **1987**, *86*, 866–872. [[CrossRef](#)]
36. Bergner, A.; Dolg, M.; Kuechle, W.; Stoll, H.; Preub, H. Ab initio energy-adjusted pseudopotentials for elements of groups 13–17. *Mol. Phys.* **1993**, *80*, 1431–1441. [[CrossRef](#)]
37. Li, Z.; Bian, K.; Zhou, M. *Excel for Windows 95 Encyclopaedia*; McFedried, P., Ed.; Electronics Industry Press: Beijing, China, 1997.
38. Sachdev, H.P.S.; Satyanarayan, L.; Kumar, S.; Puri, R.K. Classification of nutritional status as ‘Z score’ or per cent of reference median—Does it alter mortality prediction in malnourished children? *Int. J. Epiderm.* **1992**, *21*, 916–921. [[CrossRef](#)]
39. Ayatollahi, S.M.T. Age standardization of weight-for-height in children using a unified z-score method. *Ann. Hum. Biol.* **1995**, *22*, 151–162. [[CrossRef](#)]



© 2019 by the authors. Licensee MDPI, Basel, Switzerland. This article is an open access article distributed under the terms and conditions of the Creative Commons Attribution (CC BY) license (<http://creativecommons.org/licenses/by/4.0/>).